Ocean Engineering 191 (2019) 106488

Contents lists available at ScienceDirect

Ocean Engineering

journal homepage: www.elsevier.com/locate/oceaneng

# Hydrodynamic coefficient estimation for ship manoeuvring in shallow water using an optimal truncated LS-SVM

Haitong Xu, C. Guedes Soares *

*Centre for Marine Technology and Ocean Engineering (CENTEC), Instituto Superior Técnico, Universidade de Lisboa, Av. Rovisco Pais, 1049-001, Lisboa, Portugal*

ARTICLE INFO

*Keywords:*
Optimal truncated LS-SVM
Parameter estimation
Dimensionality reduction
Parameter uncertainty
Nonlinear manoeuvring model

ABSTRACT

An optimal truncated least square support vector machine (LS-SVM) is proposed for the parameter estimation of a nonlinear manoeuvring model in shallow water. A nonlinear manoeuvring model in shallow water is briefly introduced and the hydrodynamic coefficients are normalized. A series of Planar Motion Mechanism tests of the DTC ship model carried out in a towing tank with shallow water are used in the study for the estimation of the parameters of the manoeuvring model. The contribution of this paper is to propose the use of the optimal truncated LS-SVM, which is a robust method for parameter estimation that diminishes the uncertainty successfully and has a low computational cost by reducing the dimensionality of the kernel matrix. The classical least square method is also employed to estimate the parameters, and the results are compared with the optimal truncated LS-SVM. The parameter uncertainty is discussed, and the performance of the obtained nonlinear manoeuvring models is tested against a validation set that was left completely untouched during the training. The $R^2$ goodness-of-fit criterion is used to demonstrate the accuracy of the obtained models.

## 1. Introduction

A marine vessel spends most part of its lifetime navigating in deep waters, however the manoeuvrability in shallow water (Tello Ruiz et al., 2015) is critically important as ships normally have to access harbours in shallow and confined waters (Lataire et al., 2012; Maimun et al., 2011; Vantorre et al., 2017; Yoshimura, 1986; Zhou et al., 2012, 2016a). The development of numerical models makes it possible to simulate the ship trajectory in deep water (Sutulo et al., 2002; Rong et al., 2019) or ship response travelling in a confined waterway (Du et al., 2017) and shallow water (Kaidi et al., 2018). The models can also be incorporated in vessel simulators (Varela and Guedes Soares, 2015a,b), which can be used to train ship pilots.

Mathematical models are widely used to describe the dynamics of ships in deep and shallow water (Maimun et al., 2011). Many mathematical models have been proposed to meet different applications considering the trade-off between the complexity and fidelity, such as the Nomoto model (Nomoto et al., 1956), Abkowitz model (Abkowitz, 1980), MMG model (Yoshimura, 2005), vectorial model (Fossen, 2011), and a generic nonlinear manoeuvring model (Sutulo and Guedes Soares, 2015). A more comprehensive review of the ship manoeuvring models can be found in Sutulo and Guedes Soares (2011).

The effect of shallow water for manoeuvring was also discussed by Vantorre et al. (2017). Norrbin (1971) discussed consequences of finite water depth for mathematical manoeuvring. The wing theory was used to calculate the derivative of ship manoeuvring in shallow water (Inoue and Murayama, 1969). An evaluation of semi-empirical formulae for manoeuvring in shallow water was discussed by Vantorre (2001). Eloot et al. (2015) reported on efforts of validation of shallow water manoeuvring simulation through free-running tests. Benchmark data for manoeuvring in shallow water of DTC ship model have been addressed by Van Zwijnsvoorde et al. (2019). For the study on manoeuvring in the confined waterways, Computational fluid dynamics (CFD) is a very useful tool. It has also been used to study the ship manoeuvring in shallow water (Jin et al., 2016; Wang et al., 2009), bank effect (Xu et al., 2017), ship-ship interaction (Zhou et al., 2016a,b), numerical PMM test (Islam and Guedes Soares, 2018), just to name a few.

As described in the report by the Manoeuvring Committee of 24th International Towing Tank Conference (ITTC, 2005), the hydrodynamic coefficients can be obtained using captive model test, CFD calculation and system identification. System identification is one of the mature techniques for building mathematical models from measured data. As described by Sutulo and Guedes Soares (2006), captive model test is a reliable and effective method to measure the hydrodynamic forces and moments, from which the hydrodynamic coefficients in a manoeuvring

* Corresponding author.
*E-mail address:* c.guedes.soares@centec.tecnico.ulisboa.pt (C.G. Soares).

https://doi.org/10.1016/j.oceaneng.2019.106488
Received 22 September 2018; Received in revised form 14 August 2019; Accepted 22 September 2019
Available online 18 October 2019

**Nomenclature**

| | |
|---|---|
| b | Bias term |
| $h$ | Water depth [m] |
| $m$ | Mass of the ship [kg] |
| $u,v,r$ | Velocities of surge, sway, and yaw rate [m/s; rad/s] |
| $\dot{u},\dot{v},\dot{r}$ | Acceleration of the surge, sway and yaw motions [m/s$^2$; rad/s$^2$] |
| $x_G$ | Gravity centre of the ship in $x$-direction [m] |
| $y$ | Measured data |
| $\mathbf{A}$ | Kernel matrix |
| $C$ | Regularization factor |
| $I_{zz}$ | Yaw moment of inertia with Z-axis [kg m2] |
| $K(x\cdot x)$ | Kernel function |
| $N'_0, N'_{uv}, N'_{ur}, \cdots$ | Nondimensionalized hydrodynamic coefficients of yaw motion |
| $R^2$ | The goodness of fit criterion |
| $\boldsymbol{S}$ | Training set |
| $T$ | Draft of the ship [m] |
| $L_{PP}$ | Length between perpendiculars [m] |
| $U$ | Speed over ground [m/s] |
| $\mathbf{U}$ | Left-singular matrix |
| $\mathbf{V}$ | Right-singular matrix |
| $\mathbf{U}_r$ | Truncated left-singular matrix |
| $\mathbf{V}_r$ | Truncated right-singular matrix |
| $\mathbf{V}_y$ | Diagonal matrix of variances of y |
| $\mathbf{V}_{\widehat{\theta}}$ | Error propagation matrix |
| $\boldsymbol{X}$ | Matrix containing measured data |
| $X, Y, N$ | Dimensioned external surge and sway force, yaw moment [N; N m] |
| $X'_0, X'_{uu}, X'_{uuu}\cdots$ | Nondimensionalized hydrodynamic coefficients of surge motion |
| $\mathbf{Y}$ | Output matrix |
| $Y'_0, Y'_{uv}, Y'_{ur}, \cdots$ | Nondimensionalized hydrodynamic coefficients of sway motion |
| $\widehat{y}(x,\widehat{\theta})$ | Estimation values |
| $\beta$ | Drift angle [rad] |
| $\boldsymbol{\theta}$ | Hydrodynamic coefficients matrix |
| $\widehat{\theta}$ | Estimated Hydrodynamic coefficients matrix |
| $\boldsymbol{w}$ | Weight matrix |
| $\rho$ | Density of water [kg/m$^3$] |
| $\mathscr{L}(\mathbf{w},b,e_i,\alpha_i)$ | Lagrange function |
| $\mu_{11},\mu_{22},\mu_{66}$ | Added mass and moment of inertia [kg; kg m$^2$] |
| $\mu_{26}$ | Cross-inertial due to sway and yaw motion [kg m$^2$] |
| $\sum_{i=1}^{N} e_i^2$ | Empirical error |
| $\Sigma$ | Singular values matrix |
| $\Sigma_r$ | Truncated singular values matrix |
| $\boldsymbol{\varphi}(x)$ | Mapping function |
| $\chi^2(\theta)$ | Chi-squared errors |

model can be identified. Least Square (LS) method is one of the most widely used identification technology because it can provide the theoretical solution if the data is ideal and rich enough to activate the dynamic of the system. Golding et al. (2006) used the least square method to estimate the nonlinear viscous damping matrix of a marine surface vessel. Ross et al. (2015) estimated the hydrodynamic coefficients of a nonlinear manoeuvring model based on Planar Motion Mechanism (PMM) tests using the nonlinear least square method. The obtained manoeuvring model was then validated in full scale (Hassani et al., 2015).

Sutulo and Guedes Soares (2014) developed an optimal offline system identification method combined the least square with genetic algorithm for the parameter estimation of a nonlinear manoeuvring mathematical model. A similar study can also be found in Xu et al. (2018b), where a loss function considering both the bias and variance of the errors between the reference outputs and the mathematical model outputs was proposed for the estimation of the hydrodynamic coefficients based on free-running manoeuvring tests. Perera et al. (2015, 2016) applied the extended Kalman filter to estimate the dynamic parameters of a modified Nomoto model for vessel steering. An online least square support vector machine was applied to modelling the nonlinear ship steering motion in real-time in Xu et al. (2019b).

However, the drawbacks, such as sensitivity to outliers, overfitting and non-consistent estimations (Golub and Reinsch, 1970), limit the application of the least square method. In order to have a robust estimation, truncated singular value decomposition (TSVD) (Chan and Hansen, 1990) has solved the ill-conditioned problem of the least square method (Hansen, 1998). TSVD can diminish the parameter uncertainty by neglecting the smaller singular values (Bell et al., 1978). The matrix corresponding to smaller singular values usually imposes more uncertainty in the process of parameter estimation. Söderström (2013), used a regularized least-square method to estimate the parameters using large datasets. Tikhonov regularization (Golub et al., 1999) was also used for solving the ill-posed problems. It can significantly improve the condition number by modifying the normal equations in the least square method while leaving the estimated parameter relatively unchanged. The effect of Tikhonov regularization is to estimate the parameters while also keeping them near the reference values (Hansen and O'Leary, 1993; Ma et al., 2017).

Recently, a kernel-based machine learning method, Support Vector Machine (SVM), proposed by Vapnik (1995), have been used for regression (Suykens et al., 2002; Vapnik, 1998). It can also be considered a special case of Tikhonov regularization (Golub et al., 1999) as it solves the optimization problem by searching the maximum-margin hyperplane, which separates the data points. Least square support vector machine (*LS-SVM*) is a modified version of SVM proposed by Suykens and Vandewalle (1999). By including the regularized square error term in the SVM, the solutions can be obtained by solving a set of linear equations instead of a convex quadratic programming (QP) problem for classical SVMs, but the drawback is that the LS-SVM loses the sparseness feature (Chen and Zhou, 2018). SVM has been used to identify the hydrodynamic coefficients for marine vessels. In (Luo and Zou, 2009), a least square support vector machine (LSSVM) was used to estimate the hydrodynamic coefficients of an Abkowitz model. Further work on this topic can be found in (Luo et al., 2016), in which, Particle Swarm Optimization was employed to choose the regularization factor. Xu and Guedes Soares (2016), used a least square support vector machine (LS-SVM) to identify a nonlinear steering model for ship autopilot design and further studies can be found in Xu and Guedes Soares (2018). Hydrodynamic parameters of a catamaran were estimated using SVM by Luo et al. (2014). The revised version of support vector regression was also employed to describe the motion of floating structures, such as, $\varepsilon$-support vector regression (Hou and Zou, 2016), nu-support vector machine (Wang et al., 2019), among thers. Zhu et al. (2017), used an optimal LS-SVM combined with artificial bee colony algorithm to estimate a dynamic model of a large container ship.

Parameter uncertainty is always an interesting topic for system identification. The identified parameter with a large uncertainty is sensitive to the noise and the corresponding model usually has a poor generalization performance. For ship manoeuvring modelling, this phenomenon, called parameter drift, is discussed in (Hwang, 1980; Luo et al., 2016; Luo and Li, 2017), where the parameter drifts from the true values when estimating the hydrodynamic coefficients, so that the obtained manoeuvring model fails to predict the manoeuvrability of the

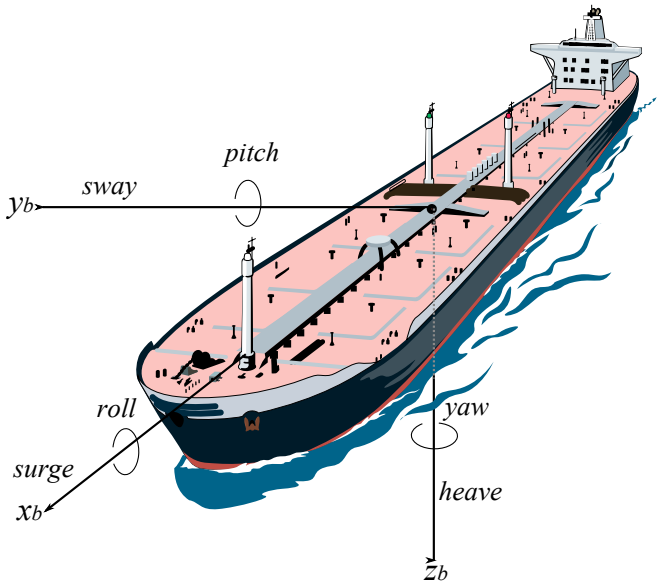


**Fig. 1.** The 6 DOFs motions of a marine surface ship in waves.

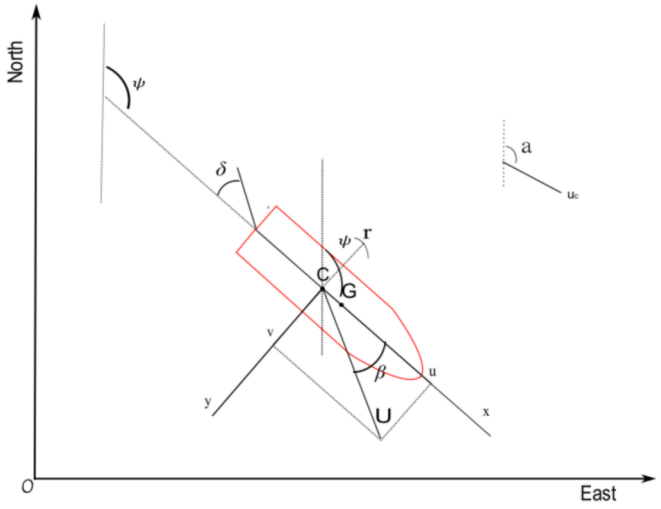


**Fig. 2.** Coordinate frames for marine surface vehicle.

ship. Hwang (1980), found the dynamic cancellation and the linear hydrodynamic coefficients drift simultaneously, using slender-body theory.

Several methods were proposed to reduce the parameter drift, such as model simplification, parallel processing and additional excitation (Luo and Li, 2017). It needs to be pointed out that the main purpose of these methods is to reconstruct the samples and reduce the multicollinearity, as the multicollinearity was considered the main reason for the parameter drift (Luo and Li, 2017). Multicollinearity is commonplace in regression analysis, and it is mostly due to the redundancy of the structure of the model (Sutulo and Guedes Soares, 2011). It is also called the ill-posed problem (Bell et al., 1978; Hansen, 1998). Xu et al. (2018a, 2019a), used the singular value decomposition to give an explanation of the parameter uncertainty. The least square methods combined with truncated singular value decomposition was used to reduce the parameter uncertainty and provide good results.

The main contribution of this paper is to propose an optimal truncated least square support vector machine (LS-SVM), and then use it to estimate the nondimensionalized coefficients of nonlinear manoeuvring models based on captive model tests. A series of PMM tests, such as pure drift, pure sway, pure yaw and mixed yaw and drift, were carried out by Flanders Hydraulics Research (FRH) in their towing tank using the DTC ship model (Moctar et al., 2012) and they are used here. The optimal truncated LS-SVM is implemented by calculating the singular value decomposition (SVD) of the kernel matrix and neglecting the small singular values as well as the corresponded matrix due to their negligible contribution to the solutions. The dimensionality reduction of the kernel matrix is achieved, which reduce the computation cost. It is different from the method in (Wei et al., 2006; Zheng et al., 2014), where singular value decomposition (SVD) was employed for signal pre-processing, and the filtered data was then used for training the classical LS-SVM. The optimal constant is estimated using *L-curve*, which plays the trade-off between the size of a regularized solution and its fit to the given data. In order to verify the results of the optimal truncated LS-SVM, classical least square method was also employed to estimate the parameters. The parameter uncertainty is discussed, and the generalization performance of the resulted numerical models are further tested against the validation set.

The structure of this article is as follow. Section 2 describes a generic nonlinear manoeuvring model for the marine surface vessel in the shallow water. In section 3, Planar Motion Mechanism (PMM) Test in shallow water carried out using DTC ship model are discussed. The classical Least Square method and optimal truncated LS-SVM are proposed in section 4. In section 5, the nondimensionalized hydrodynamic coefficients for nonlinear manoeuvring model are estimated using the classical Least Square method and optimal truncated LS-SVM. The parameter uncertainty analysis and validation are also carried out in this section. The final section is the conclusion.

## 2. Generic nonlinear manoeuvring model for marine surface vessel

Usually, the motions of a marine surface vessel can be described in six degrees of freedoms (DOFs), as illustrated in Fig. 1. They are the surge, sway, heave, roll, pitch and yaw. For ship manoeuvring, the motions in 3 DOFs (surge, sway and yaw) are considered because they typically occur with a much lower frequency than the wave encounter frequencies (Sutulo and Guedes Soares, 2011). So, it is reasonable to neglect the fluid-memory effects (Fossen, 2011). Assuming a ship moving in a horizontal plane, as presented in Fig. 2, two different coordinate systems, *North-East-Down* (*NED*) and body-fixed frame, are defined. The NED frame describes the horizontal coordinate plane and consists of three coordinates, one represents the position along the northern axis, one along the local eastern axis, and one represents the vertical position. The body frame is a moving coordinate frame that is fixed to the craft. The manoeuvring mathematical model is usually defined in the body-fixed frame. Here, it was assumed that the shallow water will affect the manoeuvrability of a ship by changing the manoeuvring coefficients. So, a generic nonlinear manoeuvring model for the marine surface vessel is given first. Without loss of generality, any marine ships can be treated as a free rigid body moving under the action of the external forces and moments. The Euler equations of arbitrary motion in the horizontal plane are given:

$$\begin{aligned}&(m+\mu_{11})\dot{u}-mvr-mx_Gr^2=X\\&(m+\mu_{22})\dot{v}+(mx_G+\mu_{26})\dot{r}+mur=Y\\&(mx_G+\mu_{26})\dot{v}+(I_{zz}+\mu_{66})\dot{r}+mx_Gur=N\end{aligned}\tag{1}$$

where, $m$ and $I_{zz}$ are the mass and the moment of inertia, respectively. $x_G$ is the position of centre-of-mass in $x$-direction. $\mu_{11}$, $\mu_{22}$ and $\mu_{26}$ are the added masses and moments, respectively. $X$, $Y$ and $N$ are the hydrodynamic forces and moment of the ship hull.

Here, the quasi-polynomials are employed to approximate the hydrodynamic forces and moments, because the quasi-polynomials can be slightly more economical from the viewpoint of the number of terms and computation speed, even if the corresponding response surface is not

**Table 1**
Dimensional factors for nondimensionalized the hydrodynamic coefficients.

| Coef. | Dimensional Factor | Coef. | Dimensional Factor | Coef. | Dimensional Factor |
|---|---|---|---|---|---|
| $\mu'_{11}$ | $0.5\rho L^2T$ | $\mu'_{22}$ | $0.5\rho L^2T$ | $\mu'_{66}$ | $0.5\rho L^4T$ |
| $X'_0$ | $0.5\rho LTU^2$ | $\mu'_{26}$ | $0.5\rho L^3T$ | $N'_0$ | $0.5\rho L^2TU^2$ |
| $X'_{vv}$ | $0.5\rho LT$ | $Y'_0$ | $0.5\rho LTU^2$ | $N'_v$ | $0.5\rho L^2TU$ |
| $X'_{vr}$ | $0.5\rho L^2T$ | $Y'_v$ | $0.5\rho LTU$ | $N'_r$ | $0.5\rho L^3TU$ |
| $X'_{rr}$ | $0.5\rho L^3T$ | $Y'_r$ | $0.5\rho L^2TU$ | $N'_{r\|v\|}$ | $0.5\rho L^3T$ |
| | | $Y'_{v\|v\|}$ | $0.5\rho LT$ | $N'_{v\|r\|}$ | $0.5\rho L^3T$ |
| | | $Y'_{v\|r\|}$ | $0.5\rho L^2T$ | $N'_{r\|r\|}$ | $0.5\rho L^4T$ |

smooth everywhere (Sutulo and Guedes Soares, 2011). The mathematical model for surge, sway and yaw motion are given:

$$X'(v',r') = X'_0 + X'_{vv}v'v' + X'_{vr}v'r' + X'_{rr}r'r' \tag{2}$$

$$Y'(v',r') = Y'_0 + Y'_v v' + Y'_r r' + Y'_{v|v|}v'|v'| + Y'_{v|r|}v'|r'| \tag{3}$$

$$N'(v',r') = N'_0 + N'_v v' + N'_r r' + N'_{r|v|}r'|v'| + N'_{v|r|}v'|r'| + N'_{r|r|}r|r| \tag{4}$$

In order to compare the coefficients of different ships and to estimate the dynamics of a full-size ship, the hydrodynamic parameters need to be converted to dimensionless ones. The prime system recommended by SNAME (1950) will be used to normalize the hydrodynamic coefficients. The water density, $\rho$, the ship length $L$ and the ship speed $U$ are employed as the characteristic dimensional parameter. The forces are normalized with $0.5\rho U^2LT$ and the moment with $0.5\rho U^2L^2T$, where $T$ is the draft at the midship. The nondimensionalized velocities and yaw rate are: $u' = u/U$, $v' = v/U$, $r' = rL/U$. The list of the nondimensionalization factors and corresponding coefficients in Eqs. (2)–(4) is shown in Table 1.

## 3. Planar motion mechanism (PMM) tests in shallow water

This section will give an overview of the planar motion mechanism (PMM) tests that have been performed by Flanders Hydraulics Research (FHR) (Delefortrie and Vantorre, 2007), in the framework of the SHOPERA project (Papanikolaou et al., 2016) test. The Duisburg Test Case (DTC) is a scaled ship model of a modern container carrier, that is used for benchmarking and validation of numerical methods (Eloot et al., 2016; Moctar et al., 2012). In total, 102 PMM tests (pure drift, pure sway and pure yaw) have been performed with different water depths, velocities, amplitudes, and sample period. In Table 2, the ranges of the main kinematic parameters, such as forward speed, drift angle, rate of turn etc. are given. The main particulars are given in Table 3. Captive model tests are nowadays commonly used for modelling the ship motions (Delefortrie et al., 2016a,b; Sutulo and Guedes Soares, 2004; Vantorre and Eloot, 1998). They can provide a rich information for system identification method and get a reasonable estimation of the hydrodynamic coefficients, however, perform such tests is costly.

Here, a brief summary of different PMM tests is presented Fig. 3, such as pure drift, pure sway, pure yaw and mixed sway and yaw, which were performed at Flanders Hydraulics Research (FHR). The towing tank at FHR has a total length of 87.5 m, a width of 7 m and a maximum water depth of 0.5 m (Eloot et al., 2016). More detailed information can be found in (Van Kerkhove et al., 2009) and (Delefortrie et al., 2016). The ship and tank fixed coordinate system is presented in Fig. 4.

In the pure drift test, the ship mode was towing forward at a constant speed with a fixed drift angle $\beta$, as presented in Fig. 5a. So, the surge and sway velocity are a non-zero constant, while the yaw rate is zero ($u = U\cos(\beta), v = U\sin(\beta), r = 0$). With the results of pure drift, the hydrodynamic coefficients related to the yaw motion can be neglected during the parameter estimation process.

Pure sway test can provide a rich information for the dynamic of the sway motion. Meanwhile, it can be used to isolate the sway dynamics from the yaw motion. During the test, the ship will move forward with a constant velocity and with a sinusoidal oscillation in sway, where $u =$

**Table 3**
The main particulars of the DTC ship model (1:89.11). cf. Ref. (Eloot et al., 2016).

| Particular | Description |
|---|---|
| Length between pp (Lpp) | 3.984 m |
| Draught (T) | 0.163 m |
| Beam (B) | 0.572 m |
| Block coefficient (Cb) | 0.661 |
| Mass | 242.8 kg |
| centre of gravity in $x$-direction ($x_G$) | −0.052 m |
| centre of gravity in $z$-direction ($z_G$) | −0.059 m |
| Moment of inertia along $x$ axis ($I_{xx}$) | 14 kg m$^2$ |
| Moment of inertia along $y$ axis ($I_{yy}$) | 212 kg m$^2$ |
| Moment of inertia along $z$ axis ($I_{zz}$) | 219 kg m$^2$ |
| Metacentric height ($\overline{GM}$) | 0.058 m |

**Fig. 3.** Planar motion mechanism tests (PMM) in a towing tank. cf. Ref. (SHOPERA, 2013-2016).

**Table 2**
The Planned test matrix in FHR cf. Ref. (SHOPERA, 2013-2016).

| Type | Water Depth[a)] | Velocity[b)] | Drift[c)] | Amplitude[d)] | Period[e)] | Number[f)] |
|---|---|---|---|---|---|---|
| Pure Drift | 2 | 3 | 7 | – | – | 28 |
| Pure Sway | 2 | 3 | 7 | 1 | 4 | 12 |
| Pure Yaw | 2 | 3 | 7 | 3 | 2 | 62 |

[a] Water Depth: 0.3254 m, 0.1952m.
[b] Velocity (Full scale): 6kn, 11kn, 16kn.
[c] Drift angle: $0^\circ, \pm2.5^\circ, \pm5^\circ, \pm10^\circ$.
[d] The amplitude of oscillation motions: Pure sway: 0.2 m; Pure yaw: $5^\circ, 10^\circ, 15^\circ$.
[e] Period (s): Pure sway: 20, 40, 60 80; Pure yaw: 17, 25.
[f] A total number of PMM test: 102.

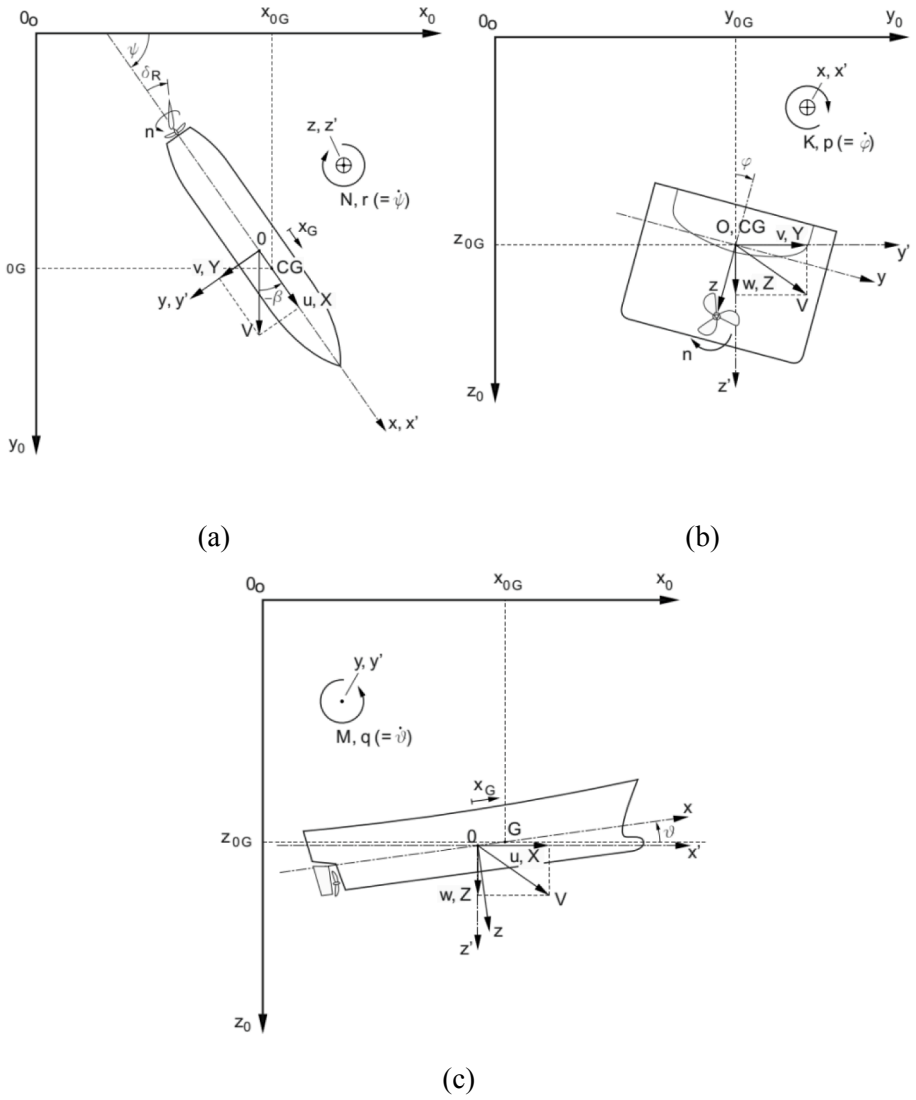


**Fig. 4.** Ship and tank fixed coordinate systems: (a)- projections on the ($x_0$, $y_0$) plane; (b)- projections on the ($y_0$, $z_0$) plane; (c)- projections on the ($x_0$, $z_0$) plane. cf. Ref. (Eloot et al., 2016).

$u_c$, $v = v_{\max}\cos(\omega t)$ and $\psi = 0$, as presented in Fig. 5b. The hydrodynamic coefficients related to the yaw motion can be neglected during the identification process because the yaw rate is zero.

Pure yaw test is used to get a full response of sway motion. During the test, the ship moves forward with a constant velocity and with a sinusoidal oscillation in sway motion, where $u = u_c$, $v = 0$ and $\psi = \psi_{\max}\sin(\omega t)$, as presented in Fig. 5c.

A combined test, pure yaw and drift, was carried out using a ship model with a sinusoidal oscillation in sway motion, as well as a sinusoidal oscillation of yaw motion around a constant drift angle. The pathline is presented in Fig. 5d. This test can provide the dynamics information of surge, sway and yaw motion. So, it can be used to estimate the coupled coefficients, which corresponded to the surge, sway and yaw motion. During the test, the ground speed and drift angle are kept as constant, and yaw rate is set as a sinusoidal oscillation, $U = U_c$, $\beta = \beta_c$ and $\psi = \psi_{\max}\sin(\omega t)$.

## 4. Parameter estimation methods and parameter uncertainty analysis

In this section, two parameter estimation methods, classical least square (LS) and least square support vector machine (LS-SVM), are introduced briefly. Then, a robust version, truncated LS-SVM, is proposed by including singular value decomposition technology. The truncated LS-SVM trains the model by calculating the singular values decomposition of the kernel matrix and neglect the smaller singular values and corresponding columns of the left-singular matrix ($\boldsymbol{U}$) and right-singular matrix ($\boldsymbol{V}$). It can reduce the computation cost due to the dimensionality reduction of the kernel matrix, meanwhile providing a robust estimation.

### 4.1. Classical least square method

In order to estimate the nondimensionalized hydrodynamic coefficients, the above equations (2)–(4) need to be reordered in a vector format given by:

$$\mathbf{X}\theta = y \tag{5}$$

where the matrix $\mathbf{X}$ contains the measured data. $\theta$ is the parameter matrix described in equation (6), and $y$ is the matrix of the hydrodynamic forces and moments. Obviously, this parameter estimation problem is over-determined, because the length of the training data, ($n$), is bigger than the number of the parameters ($n > m$). The vectors of parameters are given:

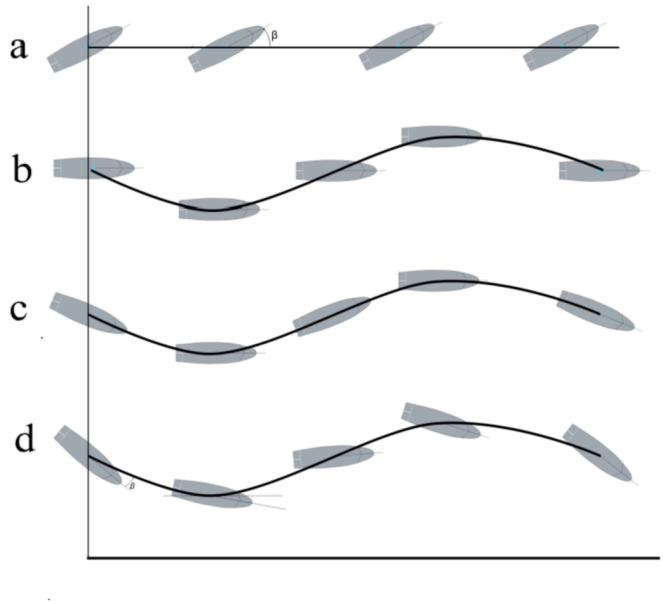


**Fig. 5.** PMM test of ship model travelling along the pathline: (a) pure drift; (b) pure sway; (c) pure yaw; (d) pure yaw + drift.

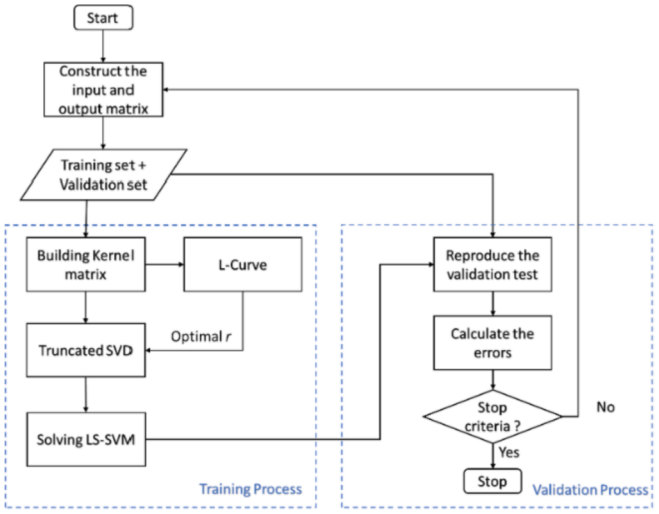


**Fig. 6.** Flowchart of optimal truncated LS-SVM

**Table 4**
The condition number of the kernel matrix of the surge, sway and yaw model.

| | Surge | Sway | Yaw |
|---|---|---|---|
| LS | 6.13E+04 | 2.67E+05 | 4.64E+04 |
| Truncated LS-SVM | 8.14E+08 | 8.38E+09 | 1.33E+11 |

$$\begin{aligned}\theta_{surge} &= \left[u_{11}^{'}, X_0^{'}, X_{vv}^{'}, X_{vr}^{'}, X_{rr}^{'}\right]\\ \theta_{sway} &= \left[\mu_{22}^{'}, \mu_{26}^{'}, Y_0^{'}, Y_v^{'}, Y_r^{'}, Y_{v|v|}^{'}, Y_{v|r|}^{'}\right]\\ \theta_{yaw} &= \left[\mu_{26}^{'}, \mu_{66}^{'}, N_0^{'}, N_v^{'}, N_r^{'}, Y_{r|v|}^{'}, N_{v|r|}^{'}, N_{r|r|}^{'}\right]\end{aligned} \tag{6}$$

Here, several assumptions need to be made. The first assumption is that the sample of measurements, $y_i$, are uncorrelated. It is reasonable because each measurement is independent. Each measurement $y_i$ has a particular variance $\sigma_y^2$, due to the environmental disturbance and sensors. Obviously, from Eq. (5), the estimation problem is to find the optimal parameter matrix, $\theta$, which can approach the measured data, $y$, or in other words, minimise the difference between the estimated values $\hat{y}(x;a)$ and the measured data $y$. The error needs to be dominated by the high-accuracy data (small-variance) and less affected by the low-accuracy data (large-variance). So, the weighted sum of the squared residuals, also called *'chi-squared'* is defined in terms of the vectors:

$$\chi^2(\theta) = (\mathbf{X}\theta - y)^T \mathbf{V}_y^{-1}(\mathbf{X}\theta - y) \tag{7}$$

where $\mathbf{V}_y$ is the diagonal matrix of variances of $y$. Usually, it can be assumed to be the identity matrix if the variances of $y$ is unknown in advance. The optimal parameters, $\theta$, corresponds to the minimum value of the $\chi^2$ error function, which means the derivative of $\chi^2$ respect to the $\theta$ equals to zero.

$$\begin{aligned}&\left.\frac{\partial \chi^2}{\partial \theta}\right|_{\theta=\widehat{\theta}} = 0\\ &\mathbf{X}^T\mathbf{V}_y^{-1}\mathbf{X}\widehat{\theta} - \mathbf{X}^T\mathbf{V}_y^{-1}y = 0\end{aligned} \tag{8}$$

Then the optimal values of the parameters can be obtained as

$$\widehat{\theta} = \left[\mathbf{X}^T\mathbf{V}_y^{-1}\mathbf{X}\right]^{-1}\mathbf{X}^T\mathbf{V}_y^{-1}y \tag{9}$$

The $\chi^2$ error function can be minimized with respect to the parameters $\theta$. The estimated values, which have the best agreement with the measured data, can be computed using $\widehat{y}(x_i;\widehat{\theta}) = \mathbf{X}\widehat{\theta}$ .

### 4.2. Optimal truncated LS-SVM and uncertainty analysis

Given the training set, which contains $N$ pairs of data, $\mathbf{S} = \{s_i | s_i = (x_i, y_i), x_i \in \Re^n, y_i \in \Re\}_{i=1}^N$, where $x_i$ is the input and $y_i$ is the output. As presented in (Suykens et al., 2002), the general approximation function of SVM is given:

$$y(x) = \mathbf{w}^T\boldsymbol{\varphi}(x) + b \tag{10}$$

where $x$ is the training samples; $y(x)$ are the target values; $b$ is the bias term; $\boldsymbol{w}$ is a weight matrix; $\boldsymbol{\varphi}(x)$ is mapping function that maps the training data, $x_i$, to a higher dimensional feature space (Suykens et al., 2002). For function estimation or regression purpose, the following optimization problem is formulated:

$$\min_{\mathbf{w},b,e_i} \qquad J(w,e) = \frac{1}{2}\mathbf{w}^T\mathbf{w} + \frac{1}{2}C\sum_{i=1}^{N} e_i^2 \tag{11}$$

subject to the equality constraints:

$$y_i = \mathbf{w}^T\boldsymbol{\varphi}(x_i) + b + e_i, \quad i = 1, \cdots, N \tag{12}$$

where $e_i, i = 1\cdots N$, is the error, and $C$ is the regularization factor. It balances the well-known structural risk, which is the trade-off between the model accuracy and the model complexity (Suykens et al., 2002). The Lagrange function is introduced to solve the optimization problem, given as:

$$\mathscr{L}(\mathbf{w}, b, e_i, \alpha_i) = \frac{1}{2}\mathbf{w}^T\mathbf{w} + \frac{1}{2}C\sum_{i=1}^{N} e_i^2 - \sum_{i=1}^{N}\alpha_i\left[\mathbf{w}^T\boldsymbol{\varphi}(x_i) + b + e_i - y_i\right] \tag{13}$$

where $\alpha_i$ are the Lagrange multipliers. According to the Karush-Kuhn-Tucker conditions (KKT) (Suykens et al., 2002), the derivatives of the Lagrange function are given by:

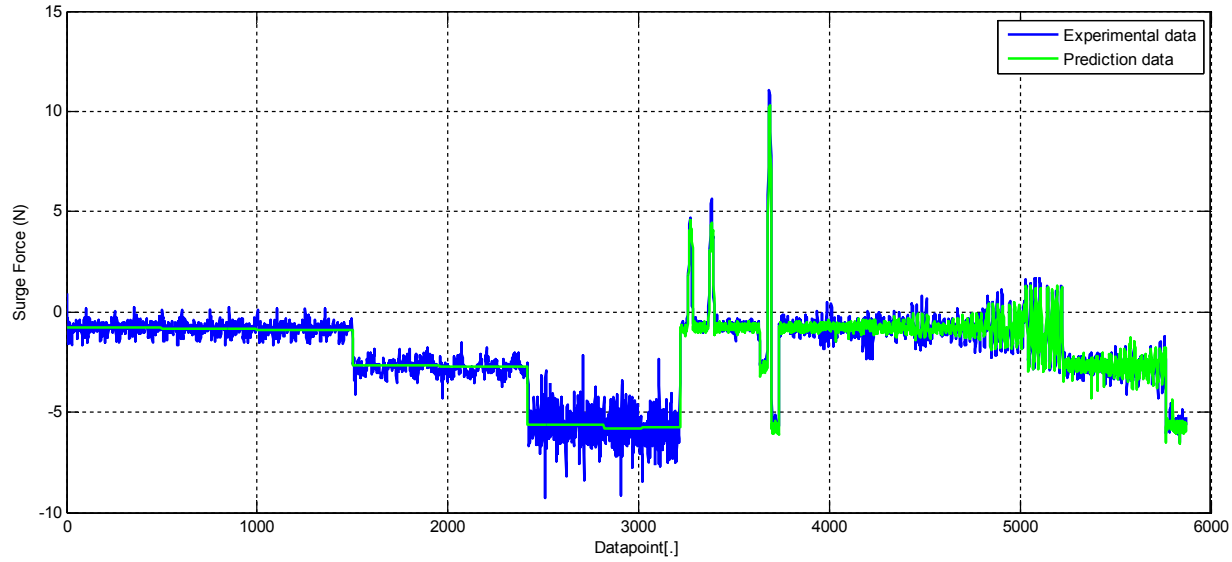


(a)

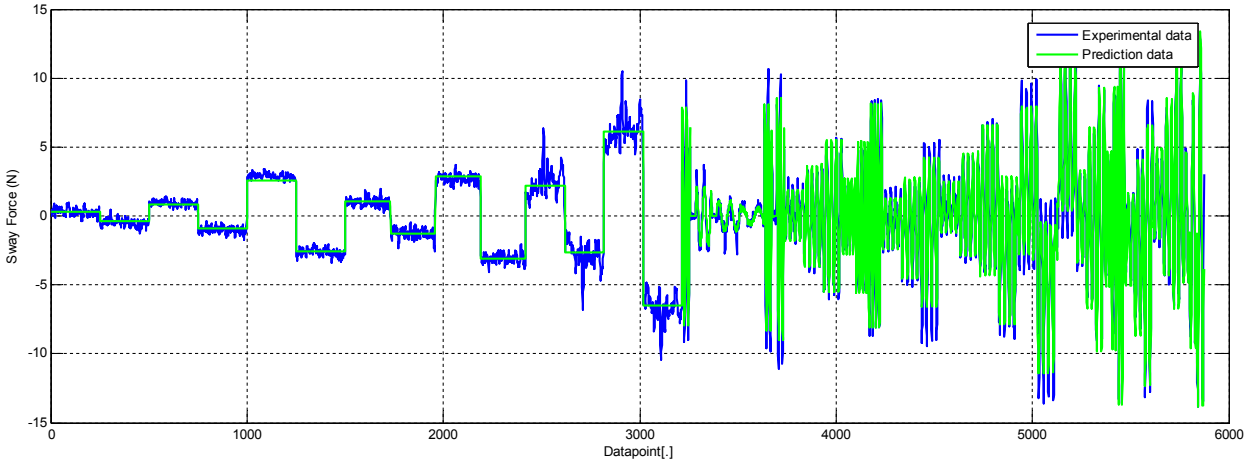


(b)

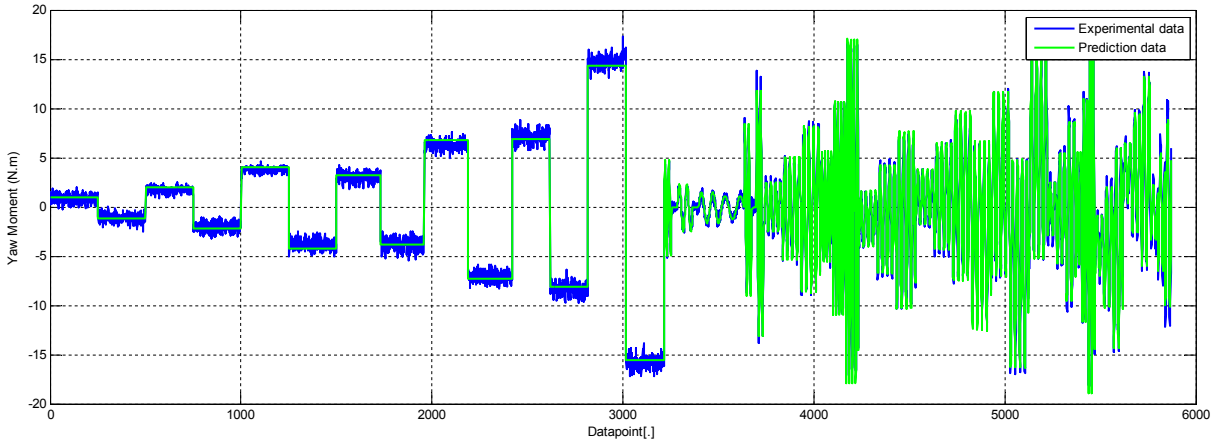


(c)

**Fig. 7.** The training process using classical Least Square method: the experiment data vs the prediction of the trained surge model (a), sway model (b), and yaw model(c).

**Table 5**
The values and deviation of the hydrodynamic coefficients of the surge model.

| Coef. | LS | | Truncated LS-SVM | |
|---|---|---|---|---|
| | Values | Deviation (%) | Values | Deviation (%) |
| $\mu'_{11}$ | 3.98E-01 | 0.58 | 3.98E-01 | 0.58 |
| $X'_0$ | −2.23E-02 | 0.36 | −2.23E-02 | 0.36 |
| $X'_{vv}$ | −1.25E-01 | 11.06 | −1.22E-01 | 11.27 |
| $X'_{vr}$ | 3.97E-01 | 2.11 | 3.97E-01 | 2.11 |
| $X'_{rr}$ | 1.06E-02 | 9.11 | 1.09E-02 | 8.89 |

**Table 6**
The values and deviation of the hydrodynamic coefficients of the sway model.

| Coef. | LS | | Truncated LS-SVM | |
|---|---|---|---|---|
| | Values | Deviation (%) | Values | Deviation (%) |
| $\mu'_{22}$ | 4.69E-01 | 0.88 | 4.69E-01 | 0.88 |
| $Y'_0$ | −8.64E-04 | 11.27 | −7.15E-04 | 13.62 |
| $Y'_v$ | −1.56E-01 | 2.83 | −1.56E-01 | 2.83 |
| $Y'_r$ | −3.81E-01 | 0.23 | −3.81E-01 | 0.23 |
| $Y'_{v\|v\|}$ | −1.55E+00 | 3.23 | −1.55E+00 | 3.23 |
| $Y'_{v\|r\|}$ | −6.83E-01 | 2.25 | −6.83E-01 | 2.25 |

**Table 7**
The values and deviation of the hydrodynamic coefficients of the yaw model.

| Coef. | LS | | Truncated LS-SVM | |
|---|---|---|---|---|
| | Values | Deviation (%) | Values | Deviation (%) |
| $\mu'_{66}$ | 3.11E-02 | 0.21 | 3.11E-02 | 0.21 |
| $\mu'_{26}$ | −6.13E-04 | 128 | −5.94E-04 | 132.51 |
| $N'_0$ | −6.62E-04 | 2.71 | −5.61E-04 | 3.19 |
| $N'_v$ | −1.73E-01 | 0.16 | −1.73E-01 | 0.16 |
| $N'_r$ | −1.69E-02 | 2.04 | −1.69E-02 | 2.03 |
| $N'_{r\|v\|}$ | −1.39E-01 | 2.73 | −1.39E-01 | 2.73 |
| $N'_{v\|r\|}$ | −8.67E-02 | 3.19 | −8.67E-02 | 3.19 |
| $N'_{r\|r\|}$ | −3.67E-02 | 1.87 | −3.66E-02 | 1.87 |

$$\begin{aligned}
&\frac{\partial \mathscr{L}}{\partial \mathbf{w}} = 0 \quad \rightarrow \quad \mathbf{w} = \sum_{i=1}^{N} \alpha_i \boldsymbol{\varphi}(x_i) \\
&\frac{\partial \mathscr{L}}{\partial b} = 0 \quad \rightarrow \quad \sum_{i=1}^{N} \alpha_i = 0 \\
&\frac{\partial \mathscr{L}}{\partial e_i} = 0 \quad \rightarrow \quad \alpha_i = Ce_i \quad i = 1, \cdots, N \\
&\frac{\partial \mathscr{L}}{\partial \alpha_i} = 0 \quad \rightarrow \quad \mathbf{w}^T \boldsymbol{\varphi}(x_i) + b + e_i - y_i = 0 \quad i = 1, \cdots, N
\end{aligned} \tag{14}$$

Eliminating the variable $\mathbf{w}$ and $e_i$, one gets the following solution:

$$\underbrace{\begin{bmatrix} 0 & \overrightarrow{1} \\ \overrightarrow{1} & K(\cdot) + C^{-1}\mathbf{I} \end{bmatrix}}_{\mathbf{A}} \underbrace{\begin{bmatrix} b \\ \overrightarrow{\alpha} \end{bmatrix}}_{\boldsymbol{\theta}} = \underbrace{\begin{bmatrix} 0 \\ \overrightarrow{Y} \end{bmatrix}}_{\mathbf{Y}} \tag{15}$$

where $\mathbf{I}$ is an $N \times N$ identity matrix. $\overrightarrow{\alpha} = [\alpha_1, \cdots \alpha_N]^T$, $\overrightarrow{Y} = [y_1, \cdots, y_N]^T$. $K(x_k \cdot x_i) = \phi(x_k)^T \phi(x_i)$, $i = 1, \cdots, N$ is the kernel function, which represents an inner product between its operands. It is positive definite and satisfies the Mercer condition (Suykens and Vandewalle, 1999; Vapnik, 1995). Here, the linear kernel function is chosen for parameter estimation. So, the resulted LS-SVM model for the regression is given:

**Table 8**
The optimal values of $r$ using *L-Curve* for the surge, sway, and yaw motion.

| | Surge | Sway | Yaw |
|---|---|---|---|
| The optimal constant ($r$) | 1764 | 942 | 961 |

**Table 9**
The $R^2$ values of the validation processes for the surge, sway and yaw motion.

| $R^2$ | Surge | Sway | Yaw |
|---|---|---|---|
| LS | 0.9460 | 0.9467 | 0.9921 |
| Truncated LS-SVM | 0.9463 | 0.9472 | 0.9930 |

$$y(x) = \sum_{i=1}^{N} \alpha_i K(x \cdot x_i) + b \tag{16}$$

As presented in Eq. (15), the dimension of the kernel matrix, $\boldsymbol{A}$, is $(N+1) \times (N+1)$. It is proportional to the length of the training set. So, if there is large data in the training set, the classical LS-SVM fails to inverse the matrix due to the heavy computation. Meanwhile, the obtained parameter matrix is usually dominated by the noise and drift from the true values. The obtained parameters do not comply with common sense. The corresponded numerical model fits well with the training data and fails to reproduce the training set. This also is well-known as overfitting. In the following phase, an optimal truncated LS-SVM is proposed to solve the parameter estimation for a large-scale problem.

Parameter uncertainty or parameter drift of the hydrodynamic coefficients was found in (Hwang, 1980; Luo and Li, 2017; Luo and Zou, 2009). The obtained parameters are usually dominated by the noise, and have large uncertainty. In (Hwang, 1980; Luo and Li, 2017), multicollinearity happens during the parameter estimation, and several methods, such as additional excitation, parallel processing, exaggerated over-and underestimation mong others, were used to diminish the parameter uncertainty. The main purpose of these methods is to reconstruct the sample and reduce the multicollinearity of variables. In this phase, parameter uncertainty is discussed using singular value decomposition. Then, a truncated least square support vector machine is proposed to diminish the parameter drift. Firstly, using the singular value decomposition, the kernel matrix, $\boldsymbol{A}$, can be rewritten as:

$$\mathbf{A} = \sum_{i=1}^{n} u_i \sigma_i v_i^T = \mathbf{U}\Sigma\mathbf{V}^T \tag{17}$$

Then, the Eq. (15) can be rewritten as:

$$\boldsymbol{\theta} = \left(\mathbf{U}\Sigma\mathbf{V}^T\right)^{-1} Y = \mathbf{V}\Sigma^{-1}\mathbf{U}^T Y = \sum_{i=1}^{n} \frac{v_i u_i^T}{\sigma_i} Y \tag{18}$$

where the matrix $\mathbf{U}$ and $\mathbf{V}$ are orthonormal, $\mathbf{U}^T\mathbf{U} = I$ and $\mathbf{V}^T\mathbf{V} = I$. $\Sigma$ is the diagonal matrix of the singular values of the matrix $\boldsymbol{X}$. Assume that there is an additive perturbation $\delta y$, then it will propagate to a perturbation in the solution,

$$\delta\theta = \mathbf{V}\Sigma^{-1}\mathbf{U}^T \delta y = \sum_{i=1}^{n} \frac{v_i u_i^T}{\sigma_i} \delta Y \tag{19}$$

As presented in Eq. (19), when the singular value, $\sigma_i$, is very small or close to the numerical precision of the computation, then the perturbation in the $y$ is magnified and potentially dominates the solutions, $\theta_i$. The corresponding columns of $\mathbf{U}$ and $\mathbf{V}$ contribute negligibly to the matrix $\boldsymbol{A}$. Their contribution to the solution can be easily dominated by the noise and round-off error in $y$. So, the obtained parameters are dominated by the noise. As discussed in the preceding section, the number of the singular, $\sigma_i$, equals to the length of the training data. The obtained parameters are inevitably dominated by the smaller singular values and are easily affected by the noise in the data and drift from the true values with a large probability. In order to diminish such

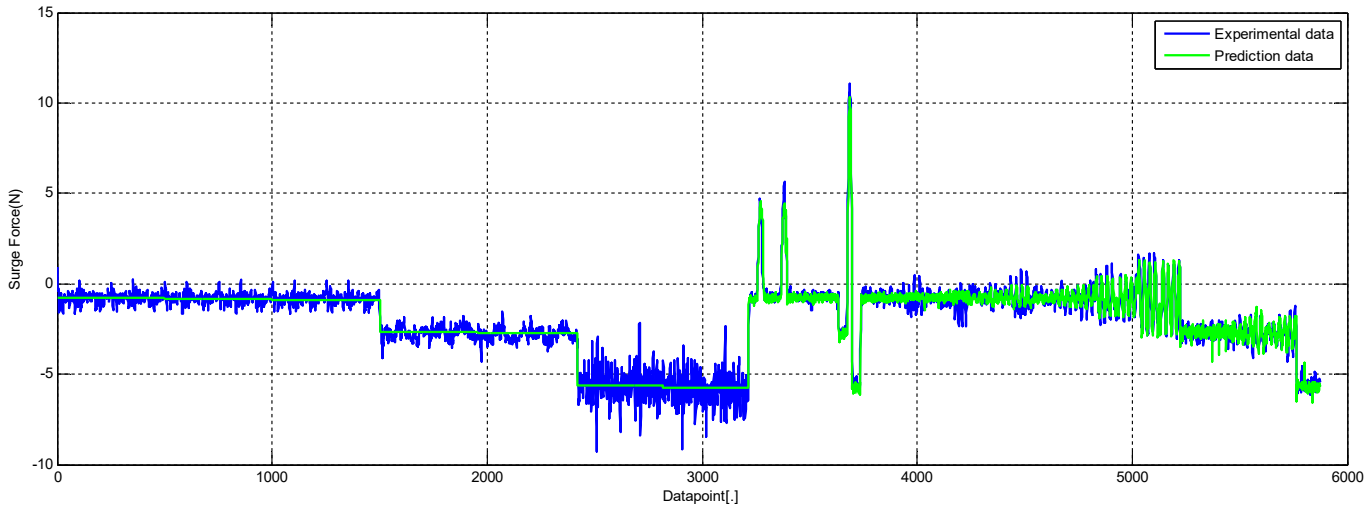
Experimental data
Prediction data
Surge Force(N)
Datapoint[.]

(a)

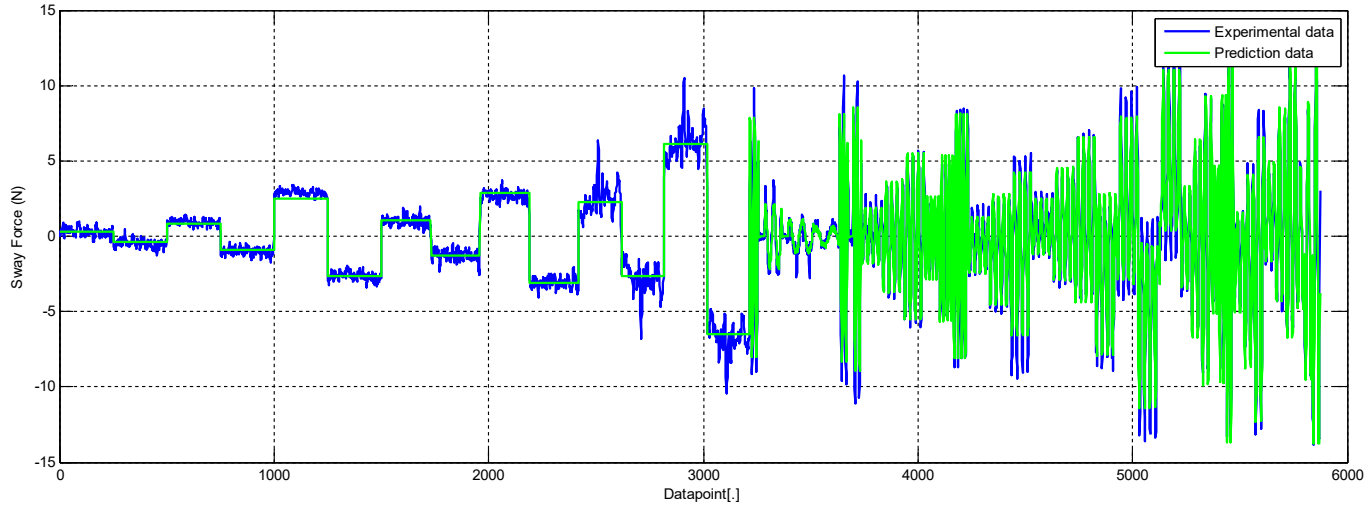
Experimental data
Prediction data
Sway Force (N)
Datapoint[.]

(b)

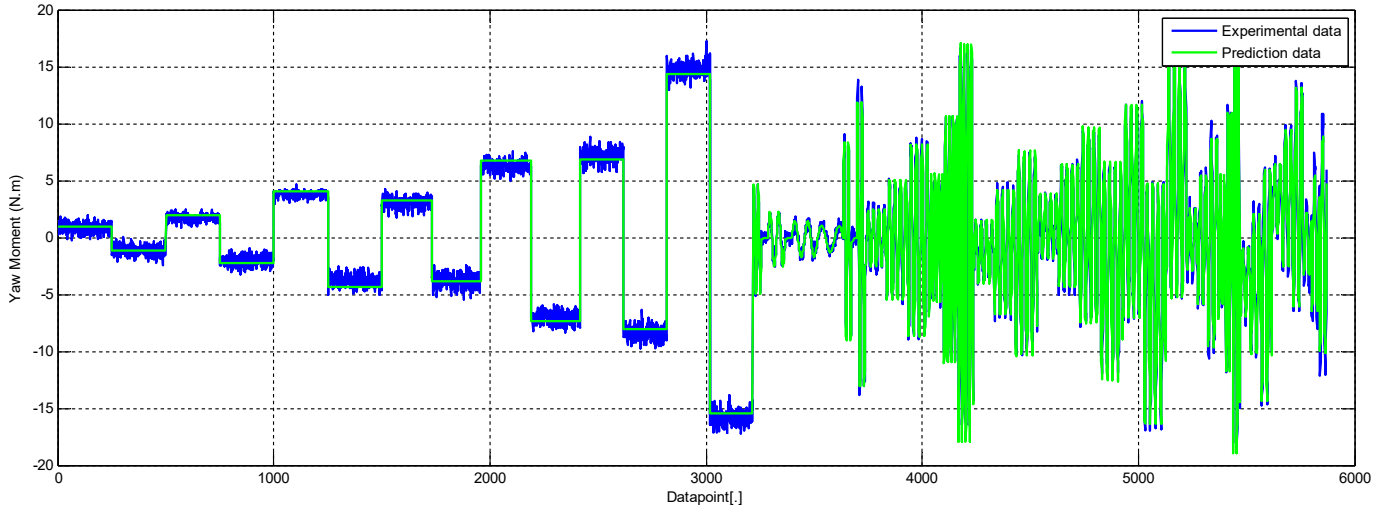
Experimental data
Prediction data
Yaw Moment (N.m)
Datapoint[.]

(c)

**Fig. 8.** The training process using optimal Truncated LS-SVM: the experiment data vs the prediction of the trained surge model (a), sway model (b), and yaw model(c).

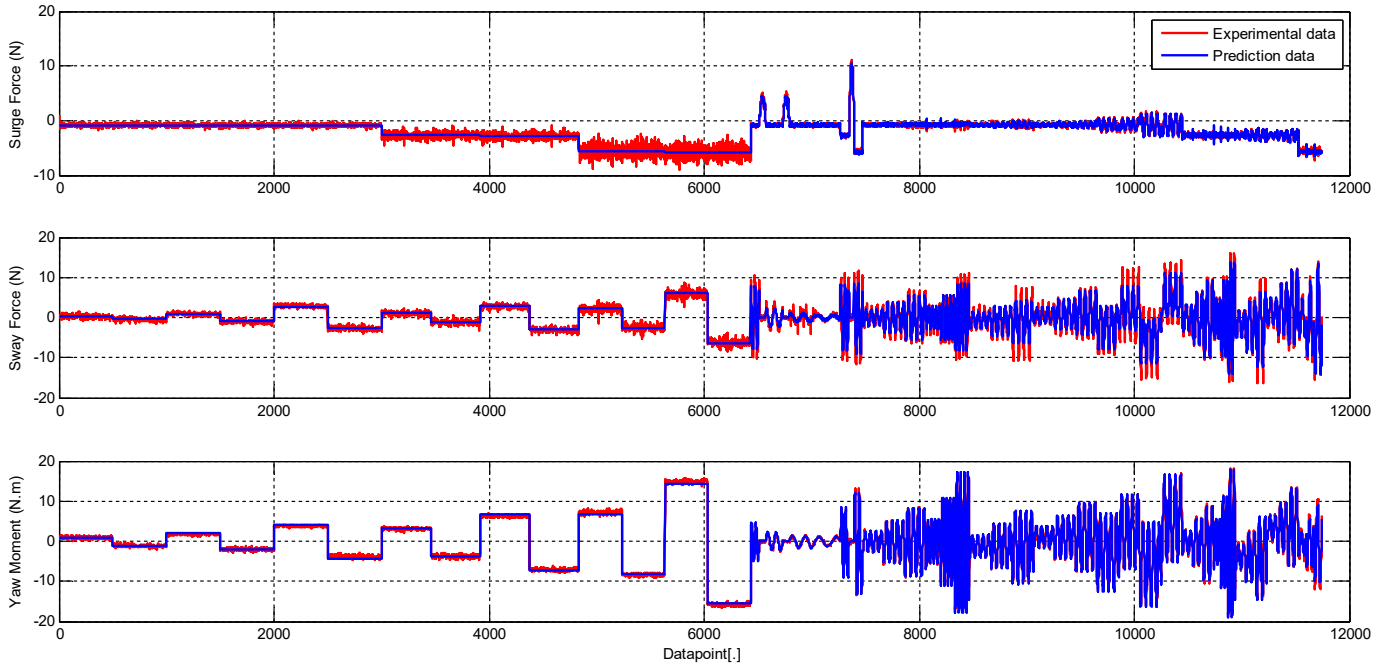


**Fig. 9.** The validation process: the experimental data vs the prediction of the obtained manoeuvring model using Least Square method (a-surge model; b-sway model; c-yaw model).

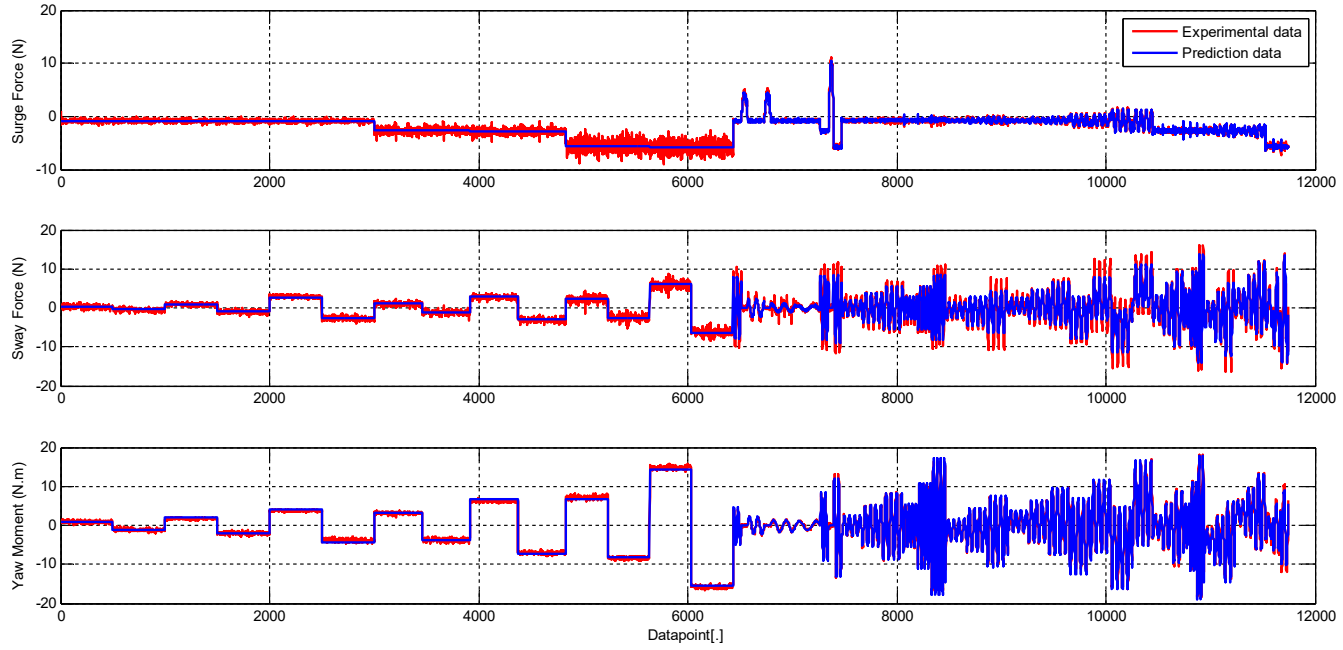


**Fig. 10.** The validation process: the experimental data vs the prediction data of the obtained manoeuvring models using optimal Truncated LS-SVM (a-surge model; b-sway model; c-yaw model).

uncertainty and obtain a robust estimation, it is necessary to neglect the effect caused by the smaller singular values. Truncated singular value decomposition (TSVD) can be used to obtain a relatively accurate representation of the matrix, $\boldsymbol{A}$, by retaining the first $r$ singular values of $\boldsymbol{A}$ and the corresponding columns of $\boldsymbol{U}$ and $\boldsymbol{V}$. The TSVD can be presented as

$$\mathbf{A}_r = \mathbf{U}_r \Sigma_r \mathbf{V}_r^T \tag{20}$$

where the matrix $\Sigma_r$ is obtained by retaining the first $r$ singular values of $\Sigma$. Similarly, matrices $\mathbf{U}_r$ and $\mathbf{V}_r$ are found using the corresponding singular vectors. The resulting $\mathbf{A}_r$ represents the reduced data set where the data related to the omitted singular values are filtered. Meanwhile,

as it can be observed, the dimensionality of the kernel matrix is reduced by using truncated singular values decomposition. The optimal value of $r$ can be estimated using the *L-curve* (Hansen and O'Leary, 1993). It is a log-log plot of the norm of a regularized solution versus the norm of the corresponding residual norm. It is a graphical tool for displaying the trade-off between the size of a regularized solution and its fit to the given data, as the $r$ varies (Golub et al., 1999; Hansen and Johnston, 2001). From the L-curve plot, it is convenient to get the optimal parameters. The whole program is given in Fig. 6.

The uncertainty of the obtained parameters is affected by noise and quantified by the error propagation matrix. The error propagation matrix or covariance matrix can be used to indicate how the random errors in $y$, as described by $\mathbf{V}_y$, propagate to the optimal parameter $\widehat{\theta}$. The error propagation matrix is given by

$$\mathbf{V}_{\widehat{\theta}} = \left[\frac{\partial \widehat{\theta}}{\partial y}\right] \mathbf{V}_y \left[\frac{\partial \widehat{\theta}}{\partial y}\right]^T \tag{21}$$

where the standard error of the parameters, $\sigma_{\widehat{\theta}}$, can get by calculation of the square-root of the diagonal of the error propagation matrix. Then the absolute error can be calculated easily.

## 5. Nondimensionalized hydrodynamic coefficients estimation and validation

In this section, the parameter estimation method discussed in the preceding section will be used to identify the nondimensionalized hydrodynamic coefficients for the nonlinear manoeuvring model. Firstly, as presented in Fig. 6, the PMM model test data will be divided into the training set and validation set for the training the model and test the generalization performance of the obtained numerical model, respectively. In order to fully activate the ship dynamics, a resampling method was used to build the training set. $x_{traning} = x(1:N:end)$, where $N$ is a constant. In order to obtain the global optimal values, the large-scale training set is chosen considering the computing power of the laptop, so N equals to 2. The length of the training set is 6000. It includes the pure drift, harmonic sway, harmonic yaw and mixed yaw and drift. For the validation, all measured data was used. The test set includes the training set and the fresh data, which is completely left untouched within the training process. The kinematic parameters of the PMM test are given in Table 2. The classical least square method and the optimal truncated least square support vector machine are both used to estimate the parameters using the training set. The uncertainty of the obtained parameters is discussed. Then, the obtained manoeuvring model will be used to reproduce the PMM tests, which are compared with the validation set.

As presented in Eq. (5), the matrix, $\mathbf{X}$ contains the measured data. If the matrix, $\mathbf{X}$, is ill-conditioned, or in the other word, the condition number is very large, then, the obtained $\widehat{\theta}$, usually contains a large uncertainty. The condition number indicates how sensitive a function is to changes or errors in the input, and how much error in the output results from an error in the input. The condition number for the Eqs. (2)–(4) is given in Table 4. Obviously, the least square support vector machine method is influenced more by the ill-conditioned matrix. As discussed in the preceding section, the dimension of the kernel matrix increases with the length of the training set, or in the other words, the number of the singular value equals to the length of the data. So, the kernel matrix is ill-conditioned with a large probability.

### 5.1. Parameter estimation using classical Least Squares method

In this phase, the classical Least Squares method will be employed to estimate the nondimensionalized hydrodynamic coefficients of the nonlinear manoeuvring model. The models for the surge, sway and yaw are given in Eqs. (2)–(4), and the parameter matrix to-be-identified is given in Eq. (6). Here, the training set contains the half of the whole PMM test data (5873 pairs data). The training set includes all the type of PMM tests, such as pure drift, pure sway, pure yaw, and mixed yaw and drift. So, it contains a rich information to excite the dynamic of manoeuvring in the shallow water.

Filtering was carried out before identification to smooth the data. The training process was carried out and the numerical prediction was compared with the experimental data, as presented in Fig. 7. Obviously, the models were trained successfully using the data, and have a good agreement with the experiment data. The obtained nondimensionalized hydrodynamic coefficients of the surge, sway and yaw model are presented in Tables 5–7, respectively, where it can be seen that most of the parameters are estimated correctly with a small deviation, except the coefficient, $\mu'_{26}$. Actually, its value is very small, so, it has a limited effect on the accuracy of the obtained numerical model. The least square method is used to minimise the sum of the squares of the residuals, so, when the training data is large, it can usually provide an optimal estimation.

### 5.2. Parameter estimation using optimal truncated LS-SVM

In this part, the optimal truncated LS-SVM is used to estimate the nondimensionalized hydrodynamic coefficients as defined in Eqs. (2)–(4). As discussed in the preceding section, the dimensions of the kernel matrix are $(N+1)\times(N+1)$, where $N$ is the length of the training set. In this paper, the number of the singular equals to 5874. In fact, most of them usually contribute negligibly to the solutions and increase the parameter uncertainty. So, it is necessary to neglect the smaller singular values.

This operation lies in two aspects: one reason is to diminish the parameter uncertainty and get a robust estimation. Another benefit is that it can reduce the dimensionality of the kernel matrix without loss of the accuracy. The most important part for truncated LS-SVM finds the optimal value of $r$, that indicates how many singular values should be kept. In this paper, a graphical tool, *L-curve* (Hansen and O'Leary, 1993), is used to obtain the optimal value. It is a log-log plot of the norm of a regularized solution versus the norm of the corresponding residual norm, which displays the trade-off between the size of a regularized solution and its fit to the given data, as the $r$ varies. More detailed introduction can be found in (Golub et al., 1999; Hansen and Johnston, 2001). From the *L-curve* plot, it is convenient to get the optimal parameters, as presented in Table 8. Only a small portion of singular values and corresponded matrix, $\mathbf{U}_r$ and $\mathbf{V}_r$ are needed to approximate the kernel matrix. So, dimensionality reduction of the kernel matrix is achieved, which reduces the computational cost (see Table 9).

The training process was carried out using the proposed method, optimal truncated LS-SVM. Fig. 8 presented the results of the trained surge (Fig. 8a), sway (Fig. 8b) and yaw motion (Fig. 8c). The resulting LS-SVM numerical model has a good agreement with the data in the training set. The obtained nondimensionalized hydrodynamic coefficients of the surge, sway and yaw model are presented in Tables 5–7 As can be observed, most of the parameters have similar values with the ones obtained using theclassical least square method. It also indicated the proposed method, optimal Truncated LS-SVM, works well with the large-scale data and provide a robust estimation. The deviation of the obtained parameters is very small, and the uncertainty is diminished successfully. The obtained values are near the true values.

### 5.3. Validation of the obtained nonlinear manoeuvring models

Once the manoeuvring models are obtained, the next most important thing is to validate whether the models are good enough to represent the dynamic of the manoeuvring. The generalization of the performance of the obtained models is usually needed to be checked using the validation data. The generalization performance or error is a measure of how

accurately a model is able to predict outcome values for previously unseen data. In this paper, the validation set includes the whole PMM test data, both the training set and the new data, which was left completely untouched during the training process.

Fig. 9 presents the surge, sway forces and yaw moment, which are reproduced based on the obtained nonlinear manoeuvring model using the classical least square method. According to the figure, the nonlinear manoeuvring model can reproduce the forces and moments during the PMM test with a good accuracy. The $R^2$ goodness-of-fit criterion is used to measure the fitness, given in Table 8. Fig. 10 shows the validation process of the nonlinear manoeuvring model, which was identified using optimal truncated LS-SVM. The forces of surge (Fig. 10a), and sway (Fig. 10b) and yaw moment (Fig. 10c) were compared with the experimental results during the PMM test and they are in good agreement. The $R^2$ values of the surge, sway and yaw model are given in Table 8, where it can be seen that the optimal truncated LS-SVM is a good option to estimate the hydrodynamic coefficients of the nonlinear manoeuvring model. The obtained model has a good generalization performance and can reproduce the PMM model test successfully.

## 6. Conclusions

An optimal truncated least square support vector machine was proposed to estimate the nondimensionalized coefficients of nonlinear manoeuvring models in shallow water. Firstly, a nonlinear manoeuvring model in 3-DOFs (surge, sway and yaw) was introduced and the hydrodynamic coefficients have been converted to the dimensionless ones using the prime system of SNAME (1950). PMM model tests, such pure drift, pure sway, pure yaw, were carried out in FHR's towing tank (Delefortrie et al., 2016a,b) using the DTC ship model in shallow water during the EU project SHOPERA (Papanikolaou et al., 2016). Optimal Truncated LS-SVM was proposed to obtain a robust parameter estimation. It reduces the dimensionality of the kernel matrix and avoids the costly matrix inversion operation by using the singular values decomposition. The smaller singular values and corresponded matrix are neglected considering their contribution to the solutions is negligible. The classical least square method was employed to estimate the parameters and the results were compared with the optimal Truncated LS-SVM. The parameter uncertainty was also discussed, and the generalization performance of the obtained nonlinear manoeuvring models was further tested against the validation set, which was completely left untouched during the training. The results show that the optimal truncated LS-SVM is a robust method for parameter estimation. The identified parameters are with a small uncertainty and can reproduce the PMM test successfully. The $R^2$ goodness-of-fit criterion was used to demonstrate the accuracy of the obtained models.

## Acknowledgements

This work was performed within the Stratc Research Plan of the Centre for Marine Technology and Ocean Engineering (CENTEC), which is financed by Portuguese Foundation for Science and Technology (Fundação para a Ciência e Tecnologia-FCT) under contract UID/Multi/00134/2013 - LISBOA-01-0145-FEDER-007629. The PMM data was collected in the experiments performed during the Project " SHOPERA-Energy Efficient Safe SHip OPERAtion " (Papanikolaou et al., 2016), which was partially funded by the EU under contract 605221. The first author is grateful to Prof. Serge Sutulo for valuable discussions on manoeuvring models.

## References

Abkowitz, M.A., 1980. Measurement of hydrodynamic characteristics from ship maneuvering trials by system identification. Trans. SNAME 88, 283–318.
Bell, J.B., Tikhonov, A.N., Arsenin, V.Y., 1978. Solutions of ill-posed problems. Math. Comput. 32, 1320.
Chan, T.F., Hansen, P.C., 1990. Computing truncated singular value decomposition least squares solutions by rank revealing QR-factorizations. SIAM J. Sci. Stat. Comput. 11, 519–530.
Chen, L., Zhou, S., 2018. Sparse algorithm for robust LSSVM in primal space. Neurocomputing 275, 2880–2891.
Delefortrie, G., Vantorre, M., 2007. Experimental studies on seakeeping and maneuverability of ships in adverse weather conditions. J. Ship Res. 51, 287–296.
Delefortrie, G., Eloot, K., Lataire, E., Van Hoydonck, W., Vantorre, M., 2016. Captive model tests based 6 DOF shallow water manoeuvring model. In: 4th MASHCON-International Conference on Ship Manoeuvring in Shallow and Confined Water with Special Focus on Ship Bottom Interaction, pp. 273–286.
Delefortrie, G., Geerts, S., Vantorre, M., 2016. The towing tank for manoeuvres in shallow water. In: 4th MASHCON-International Conference on Ship Manoeuvring in Shallow and Confined Water with Special Focus on Ship Bottom Interaction, pp. 226–235.
Du, P., Ouahsine, A., Toan, K.T., Sergent, P., 2017. Simulation of ship maneuvering in a confined waterway using a nonlinear model based on optimization techniques. Ocean Eng. 142, 194–203.
Eloot, K., Delefortrie, G., Vantorre, M., Quadvlieg, F., 2015. Validation of ship manoeuvring in shallow water through free-running tests. Ocean Eng. Volume 7. ASME, p. V007T06A017.
Eloot, K., Vantorre, M., Delefortrie, G., Lataire, E., 2016. Running sinkage and trim of the DTC container carrier in harmonic sway and yaw motion : open model test data for validation purposes. In: Uliczka, K., Böttner, C.-U., Kastens, M., Eloot, K., Delefortrie, G., Vantorre, M., Candries, M., Lataire, E. (Eds.), The 4th International Conference on Ship Manoeuvring in Shallow and Confined Water (MASHCON): Ship Bottom Interaction. Bundesanstalt für Wasserbau, Hamburg, Germany, pp. 251–261.
Fossen, T.I., 2011. Handbook of Marine Craft Hydrodynamics and Motion Control. John Wiley & Sons, Ltd, Chichester, UK.
Golding, B., Ross, A., Fossen, T.I., 2006. Identification of nonlinear viscous damping for marine vessels. In: 14 Th IFAC Symposium on System Identification. Newcastle , Australia, pp. 332–337, 2006.
Golub, G.H., Reinsch, C., 1970. Singular value decomposition and least squares solutions. Numer. Math. 14, 403–420.
Golub, G.H., Hansen, P.C., O'Leary, D.P., 1999. Tikhonov regularization and total least squares. SIAM J. Matrix Anal. Appl. 21, 185–194.
Hansen, P., 1998. Rank-deficient and discrete ill-posed problems: numerical aspects of linear inversion. Soc. Ind. Appl. Math. 175–208.
Hansen, P.C., Johnston, P.R., 2001. The L-curve and its use in the numerical treatment of inverse problems. In: Computational Inverse Problems in Electrocardiography, pp. 119–142.
Hansen, P.C., O'Leary, D.P., 1993. The use of the L-curve in the regularization of discrete ill-posed problems. SIAM J. Sci. Comput. 14, 1487–1503.
Hassani, V., Fathi, D., Ross, A., Sprenger, F., Selvik, Ø., Berg, T.E.T.E., Fathi, D., Sprenger, F., Berg, T.E.T.E., 2015. Time domain simulation model for research vessel Gunnerus. In: Proceedings of the International Conference on Offshore Mechanics and Arctic Engineering - OMAE. ASME paper V007T06A013.
Hou, X.-R., Zou, Z.-J., 2016. Parameter identification of nonlinear roll motion equation for floating structures in irregular waves. Appl. Ocean Res. 55, 66–75.
Hwang, W., 1980. Application of System Identification to Ship Maneuvering. Massachusetts Institute of Technology.
Inoue, S., Murayama, K., 1969. Calculation of Turning Ship Derivatives in Shallow Water. West Japan Soc. Nav. Archit.
Islam, H., Guedes Soares, C., 2018. Estimation of hydrodynamic derivatives of a container ship using PMM simulation in OpenFOAM. Ocean Eng. 164, 414–425.
ITTC, 2005. Final report and recommendations to the 24th ITTC. In: 24th International Towing Tank Conference, pp. 369–408.
Jin, Y., Duffy, J., Chai, S., Chin, C., Bose, N., 2016. URANS study of scale effects on hydrodynamic manoeuvring coefficients of KVLCC2. Ocean Eng. 118, 93–106.
Kaidi, S., Smaoui, H., Sergent, P., 2018. Modeling the maneuvering behavior of container carriers in shallow water. J. Waterw. Port, Coast. Ocean Eng. 144, 04018017.
Lataire, E., Vantorre, M., Delefortrie, G., Candries, M., 2012. Mathematical modelling of forces acting on ships during lightering operations. Ocean Eng. 55, 101–115.
Luo, W., Li, X., 2017. Measures to diminish the parameter drift in the modeling of ship manoeuvring using system identification. Appl. Ocean Res. 67, 9–20.
Luo, W.L., Zou, Z.J., 2009. Parametric identification of ship maneuvering models by using support vector machines. J. Ship Res. 53, 19–30.
Luo, W., Moreira, L., Guedes Soares, C., 2014. Manoeuvring simulation of catamaran by using implicit models based on support vector machines. Ocean Eng. 82, 150–159.
Luo, W., Guedes Soares, C., Zou, Z., 2016. Parameter identification of ship maneuvering model based on support vector machines and particle swarm optimization. J. Offshore Mech. Arct. Eng. 138, 031101.
Ma, D., Tan, W., Zhang, Z., Hu, J., 2017. Parameter identification for continuous point emission source based on Tikhonov regularization method coupled with particle swarm optimization algorithm. J. Hazard Mater. 325, 239–250.
Maimun, A., Priyanto, A., Muhammad, A.H., Scully, C.C., Awal, Z.I., 2011. Manoeuvring prediction of pusher barge in deep and shallow water. Ocean Eng. 38, 1291–1299.
Moctar, O. el, Shigunov, V., Zorn, T., 2012. Duisburg test case: post-panamax container ship for benchmarking. Ship Technol. Res. 59, 50–64.
Nomoto, K., Taguchi, K., Honda, K., Hirano, S., 1956. On the steering qualities of ships. J. Zosen Kiokai 75–82, 1956.
Norrbin, N.H., 1971. Theory and observations on the use of a mathematical model for ship manoeuvring in deep and confined waters. In: 8th Symposium on Naval Hydrodynamics. Pasadena.

Papanikolaou, A., Zaraphonitis, G., Bitner-Gregersen, E., Shigunov, V., Moctar, O. El, Guedes Soares, C., Reddy, D.N., Sprenger, F., 2016. Energy efficient Safe SHip operation (SHOPERA). Transp. Res. Procedia 14, 820–829.
Perera, L.P., Oliveira, P., Guedes Soares, C., 2015. System identification of nonlinear vessel steering. J. Offshore Mech. Arct. Eng. 137 (3), 031302-1 -7.
Perera, L.P., Oliveira, P., Guedes Soares, C., 2016. System identification of vessel steering with unstructured uncertainties by persistent excitation maneuvers. J Ocean. Eng. IEEE 41 (3), 515–528, 2016.
Rong, H., Teixeira, A.P., Guedes Soares, C., 2019. Ship trajectory uncertainty prediction based on a Gaussian Process model. Ocean Eng. 182, 499–511.
Ross, A., Selvik, O., Hassani, V., Ringen, E., Fathi, D., 2015. Identification of nonlinear manoeuvring models for marine vessels using planar motion mechanism tests. In: ASME 2015 34th International Conference on Ocean. Offshore and Arctic Engineering. V007T06A014-V007T06A014.
SHOPERA, 2013-2016. Energy efficient Safe SHip OPERAtion , EU project FP7-SST-2013-RTD-1, 2013-2016. http://www.shopera.org.
SNAME, 1950. Nomenclature for Treating the Motion of a Submerged Body through a Fluid. Society of Naval Architects and Marine Engineers, New York.
Söderström, T., 2013. Comparing some classes of bias-compensating least squares methods. Automatica 49, 840–845.
Sutulo, S., Guedes Soares, C., 2004. Synthesis of experimental designs of manouevring captive-model tests with large number of factors. J. Mar. Sci. Technol. 9 (1), 32–42.
Sutulo, S., Guedes Soares, C., 2006. Development of a multifactor regression model of ship maneuvering forces based on optimized captive-model tests. J. Ship Res. 50, 311–333.
Sutulo, S., Guedes Soares, C., 2011. Mathematical models for simulation of manoeuvring performance of ships. In: Guedes Soares, C., Garbatov, Y., Fonseca, N., Teixeira, A.P. (Eds.), Maritime Engineering and Technology. Taylor & Francis Group, London, pp. 661–698.
Sutulo, S., Guedes Soares, C., 2014. An algorithm for offline identification of ship manoeuvring mathematical models from free-running tests. Ocean Eng. 79, 10–25.
Sutulo, S., Guedes Soares, C., 2015. Development of a core mathematical model for arbitrary manoeuvres of a shuttle tanker. Appl. Ocean Res. 51, 293–308.
Sutulo, S., Moreira, L., Guedes Soares, C., 2002. Mathematical models for ship path prediction in manoeuvring simulation systems. Ocean Eng. 29 (1), 1–19.
Suykens, J.A.K., Vandewalle, J., 1999. Least squares support vector machine classifiers. Neural Process. Lett. 9, 293–300.
Suykens, J.A.K., Van Gestel, T., De Brabanter, J., De Moor, B., Vandewalle, J., 2002. Least Squares Support Vector Machines. World Scientific.
Tello Ruiz, M.Á., De Caluwé, S., van Zwijnsvoorde, T., Delefortrie, G., Vantorre, M., 2015. Wave effects on manoeuvring ships in shallow water. In: MARSIM 2015, Int. Conf. Sh. Manoeuvrability Marit. Simulation, 8th – 11th Sept. 2015. Newcastle Univ. United Kingdom Proc.
Van Kerkhove, G., Vantorre, M., Delefortrie, G., 2009. Advanced model testing techniques for ship behaviour in shallow and confined water. In: AMT '09 : 1st International Conference on Advanced Model Measurement Technology for the EU Maritime Industry, pp. 158–172.
Van Zwijnsvoorde, T., Manases Tello, R., Delefortrie, G., Lataire, E., 2019. Sailing in shallow water waves with the DTC container carrier: open model test data for validation purposes. In: 5th MASHCON International Conference on Ship Manoeuvring in Shallow and Confined Water. Ostend, Belgium.
Vantorre, M., 2001. Manoeuvring coefficients for a container carrier in shallow water: an evaluation of semi-empirical formulae. In: Mini Symposium on Prediction of Ship Manoeuvring Performance, 18 October 2001, Tokyo, Japan.
Vantorre, M., Eloot, K., 1998. Requirements for standard harmonic captive manoeuvring tests. Contr. Eng. Pract.
Vantorre, M., Eloot, K., Delefortrie, G., Lataire, E., Candries, M., Verwilligen, J., 2017. Maneuvering in shallow and confined water. In: Encyclopedia of Maritime and Offshore Engineering. John Wiley & Sons, Ltd, Chichester, UK, pp. 1–17.
Vapnik, V.N., 1995. The Nature of Statistical Learning Theory, vol. 8. Springer, p. 187.
Vapnik, V.N., 1998. Statistical Learning Theory. John Wiley & Sons.
Varela, J.M., Guedes Soares, C., 2015. Software architecture of an interface for three-dimensional collision handling in maritime Virtual Environments. Simulation 91, 735–749.
Varela, J.M., Guedes Soares, C., 2015. Interactive 3D desktop ship simulator for testing and training offloading manoeuvres. Appl. Ocean Res. 51, 367–380.
Wang, H., Zou, Z., Tian, X., 2009. Computation of the viscous hydrodynamic forces on a KVLCC2 model moving obliquely in shallow water. J. Shanghai Jiao Tong Univ. (Sci.) 14, 241–244.
Wang, Z., Zou, Z., Guedes Soares, C., 2019. Identification of ship manoeuvring motion based on nu-support vector machine. Ocean Eng. 183, 270–281.
Wei, T., Zhongke, S., Hongchao, L., 2006. Denoising of impulse response using LS-SVM and SVD for aircraft flight flutter test. In: Systems and Control in Aerospace and Astronautics, 2006. ISSCAA 2006. 1st International Symposium on, vol. 5. IEEE, p. 688.
Xu, H.T., Guedes Soares, C., 2016. Vector field path following for surface marine vessel and parameter identification based on LS-SVM. Ocean Eng. 113, 151–161.
Xu, H.T., Guedes Soares, C., 2018. An optimized energy-efficient path following algorithm for underactuated marine surface ship model. Int. J. Marit. Eng. 160 (A4), A413–A423.
Xu, H., Zou, Z., Wu, S., Liu, X., Zou, L., 2017. Bank effects on ship–ship hydrodynamic interaction in shallow water based on high-order panel method. Ships Offshore Struct. 12, 843–861.
Xu, H.T., Hassani, V., Guedes Soares, C., 2018. Parameters estimation of nonlinear manoeuvring model for marine surface ship based on PMM tests. In: ASME 2018 37th International Conference on Ocean, Offshore and Arctic Engineering. ASME, Madrid, Spain paper OMAE2018-78235.
Xu, H.T., Hinostroza, M.A., Guedes Soares, C., 2018. Estimation of hydrodynamic coefficients of a nonlinear manoeuvring mathematical model with free-running ship model tests. Int. J. Marit. Eng. 160 (A3), A213–A225.
Xu, H.T., Hassani, V., Guedes Soares, C., 2019. Uncertainty analysis of the hydrodynamic coefficients estimation of a nonlinear manoeuvring model based on planar motion mechanism tests. Ocean Eng. 173, 450–459.
Xu, H.T., Hinostroza, M.A., Hassani, V., Guedes Soares, C., 2019. Real-Time parameter estimation of nonlinear vessel steering model using support vector machine. J. Offshore Mech. Arct. Eng. 141 (6), 061606.
Yoshimura, Y., 1986. Mathematical model for the manoeuvring ship motion in shallow water. J. Kansai Soc. Nav. Archit.
Yoshimura, Y., 2005. Mathematical model for manoeuvring ship motion (MMG Model). In: Workshop on Mathematical Models for Operations Involving Ship-Ship Interaction. Kansai Zōsen Kyōkai Kyōkai, pp. 1–6.
Zheng, P.-P., Feng, J., Li, Z., Zhou, M., 2014. A novel SVD and LS-SVM combination algorithm for blind watermarking. Neurocomputing 142, 520–528.
Zhou, X.Q., Sutulo, S., Guedes Soares, C., 2012. Computation of ship hydrodynamic interaction forces in restricted waters using potential theory. J. Mar. Sci. Appl. 11, 265–275.
Zhou, X., Sutulo, S., Guedes Soares, C., 2016. Ship-Ship hydrodynamic interaction in confined waters with complex boundaries by a o Panelled Moving Patch Method. Int. J. Marit. Eng. 158 (Part A1):A-21 - A30.
Zhou, X., Sutulo, S., Guedes Soares, C., 2016. A paving algorithm for dynamic generation of quadrilateral meshes for online numerical simulations of ship manoeuvring in shallow water. Ocean Eng. 122, 10–21.
Zhu, M., Hahn, A., Wen, Y.-Q., Bolles, A., 2017. Identification-based simplified model of large container ships using support vector machines and artificial bee colony algorithm. Appl. Ocean Res. 68, 249–261.